Monolithically Integrated 940 nm Half VCSELs on Bulk Ge Substrates

Yunlong Zhao, Zeyu Wan, Jia Guo, Yun-Cheng Yang, Hao-Tien Cheng, *Graduate Student Member, IEEE*, Lukas Chrostowski, *Senior Member, IEEE*, David Lackner, Chao-Hsin Wu, *Member, IEEE*, and Guangrui Xia

***Abstract*— High-quality n-type AlGaAs distributed Bragg reflectors (DBRs) and lnGaAs multiple quantum wells (MQWs) were successfully monolithically grown on 4-inch off-cut Ge (100) wafers. Even without any design and process optimization for the Ge substrates, the Ge-based half VCSELs have photoluminescence and reflectance spectra comparable to those grown on conventional GaAs wafers. Flat and sub-nm RMS surface roughness and uniform DBR and MQW growth across the wafer were achieved. These results strongly support full VCSEL growth and fabrication on larger-area Ge wafers for the mass production of AlGaAs-based VCSELs.**

***Index Terms*— Distributed Bragg reflector (DBR), growth quality, optical performance, reflectance, stopband, vertical cavity surface emitting laser (VCSEL).**

I. Introduction

THE demand for vertical cavity surface emitting lasers (VCSELs) has dramatically increased in the past few years due to their applications as near-infrared illumination sources in three-dimensional (3D) sensing and imaging, powering some of the most popular features in smartphones, virtual reality (VR) and augmented reality (AR) applications, such as Face ID in iPhone and proximity-sensing [1], [2]. Compared with other laser technology, the benefits of VCSEL technology include scalable output power, high-quality optical beam, high wall-plug efficiency, stable wavelength over temperature, low spectral width, and easy testing and packaging [3]. VCSELs are also widely used in the light detection and ranging (LiDAR) system in electric vehicles and autonomous mobile robots. As a result, the global VCSEL market was predicted to increase further to $3.9 billion by 2027 from the $1.6 billion market size in 2022 [4]. Until now, VCSEL production still relies on conventional 3, 4-inch bulk GaAs wafers and shifting to 6-inch bulk GaAs wafers, limiting the production volume [5]. Scaling up the VCSEL production using larger wafers is a very effective way to solve this problem, which is especially beneficial to boosting larger VCSEL array production used in high-power LiDAR.

The primary concern in the epitaxy of AlGaAs VCSELs on GaAs substrates is the inherent strain formed during VCSEL growth [6], [7]. The thickness of a typical VCSEL epitaxial structure is commonly about 5 to 15 microns, mainly contributed by the bottom and the top distributed Bragg reflectors (DBRs) made of $Al_xGa_{1-x}As/Al_yGa_{1-y}As$ superlattices ($x < y$). GaAs (the lower limit of $Al_xGa_{1-x}As$), Ge, and AlAs (the higher limit of $Al_yGa_{1-y}As$), have lattice constants of 5.653, 5.658, and 5.660 Å, respectively. For the production of 3-inch and 4-inch GaAs wafers, the lattice mismatch induced strain, 0.14% lattice constant mismatch between AlAs and GaAs, at room temperature is acceptable [8]. When the growth is on larger GaAs wafers, this strain results in a significant bow and warp on wafers after growth, which leads to low chip yield and reliability problems. A solution by replacing bulk GaAs substrates with bulk Ge substrates was proposed. The Ge lattice constant is between that of $Al_xGa_{1-x}As$ and $Al_yGa_{1-y}As$, reducing the lattice mismatch strain and thus the bow and warp of the Ge substrates after the growth [9], which make larger diameter VCSEL substrates feasible for mass production. Ge wafers also have some other advantages, including more mechanical robustness, thinner thickness, and less density of threading dislocations (TDD), which are crucial to reducing failures and lowering the yield loss in VCSELs on large-size GaAs wafers [10]. Commercially, the price of 6-inch Ge wafers is not higher than 6-inch GaAs wafers. More importantly, Ge wafers can be made up to 12-inch diameter, while GaAs wafers are too brittle for this size. Therefore, 6 to 12-inch diameter Ge wafers are promising solutions for the mass production of VCSELs without significant fabrication cost increases. The only report on bulk Ge-based full VCSELs so far was from IQE. In 2020, IQE first demonstrated 940 nm VCSELs on a 6-inch bulk Ge wafer. Without any process optimizations of Ge-based VCSELs, they produced comparable DBR stopbands, active region photoluminescence (PL) spectra, and lasing performance as conventional GaAs-based VCSELs with less wafer bow and warp [11]. However, it was unclear about their Ge substrate specifications, transition layers

Manuscript received 15 September 2023; revised 27 November 2023; accepted 4 December 2023. Date of publication 18 December 2023; date of current version 29 December 2023. This work was supported by Huawei Technologies Canada. *(Corresponding author: Guangrui Xia.)*

Yunlong Zhao, Zeyu Wan, Jia Guo, and Guangrui Xia are with the Department of Materials Engineering, The University of British Columbia (UBC), Vancouver, BC V6T 1Z4, Canada (e-mail: gxia@mail.ubc.ca).

Yun-Cheng Yang and Hao-Tien Cheng are with the Graduate Institute of Electronics Engineering, National Taiwan University, Taipei 10617, Taiwan.

Lukas Chrostowski is with the Department of Electrical and Computer Engineering, The University of British Columbia (UBC), Vancouver, BC V6T 1Z4, Canada.

David Lackner is with the Fraunhofer Institute for Solar Energy Systems (ISE), 79110 Freiburg im Breisgau, Germany.

Chao-Hsin Wu is with the Graduate Institute of Photonics and Optoelectronics, and the Graduate School of Advanced Technology, National Taiwan University, Taipei 10617, Taiwan.

Color versions of one or more figures in this letter are available at https://doi.org/10.1109/LPT.2023.3344355.

Digital Object Identifier 10.1109/LPT.2023.3344355

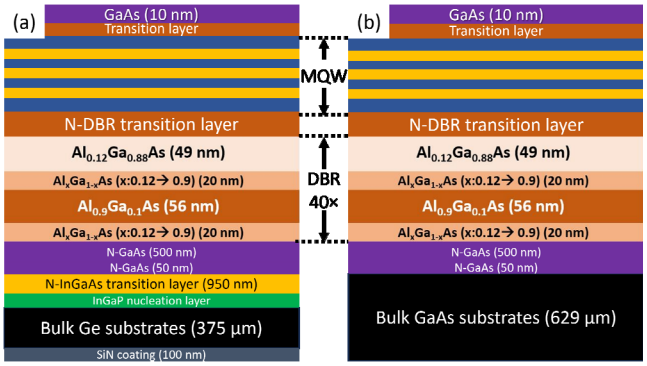

Fig. 1. Schematic structure of the half VCSELs grown on (a) GaAs/InGaAs/InGaP/Ge/SiN substrate and (b) bulk GaAs substrates.

from Ge to the AlGaAs bottom DBR, growth, and testing conditions. Later, we achieved the successful monolithic integration of $Al_xGa_{1-x}As$ n-type distributed Bragg reflectors (n-DBRs) on bulk Ge substrates independently, with an InGaP nucleation layer, InGaAs, GaAs transition layers on bulk Ge [12]. SiN backside coating was needed to prevent Ge sublimation. The n-DBRs on GaAs/InGaAs/InGaP/bulk-Ge/SiN substrates have stopbands and smooth surface morphology comparable to bulk GaAs-based DBRs [12].

Since then, we have continued to develop the epitaxy toward bulk Ge-based full VCSELs. In this work, the monolithic integration of $In_xGa_{1-x}As$ multiple quantum wells (MQW) and $Al_xGa_{1-x}As$ n-DBRs (referred to as half VCSELs thereafter) on 4-inch Ge full wafers was investigated. MQWs are the light emission layers, where alloy composition, thickness, strain, crystal quality, and the wavelength matching between the n-DBR and MQW are all crucial to the laser emission wavelength and intensity, which were addressed in this work. We report that the bulk Ge-based half VCSELs produced comparable photoluminescence and n-DBR stopband features as the GaAs counterparts. Key material, processing, and testing conditions are discussed in detail.

II. Experiment Design and Epitaxy Growth

The schematic structure of the half VCSELs on Ge substrates is illustrated in Fig. 1. The Ge substrates in this study were n-type 4-inch (100) Ge wafers with 375 μm thickness and 6-degree off-cut towards <111>. The Ge wafers were provided by Umicore. Compared with the 4-inch GaAs wafers with 629 μm thickness, the Ge wafers are much thinner of the same size due to their mechanical robustness. The off-cut prevents the formation of antiphase domains (APDs) in the subsequent GaAs layers on Ge and improves step-flow growth. Thin films of 100 nm SiN were deposited on the Ge wafer backsides to prevent Ge sublimation during high-temperature processes.

To transition from the Ge wafers, an InGaP nucleation layer, a 950 nm n-$Ga_{0.985}In_{0.015}As$ layer with the lattice constant matched to Ge, and a 50 nm n-GaAs layer with 5×10^{18} cm^{-3} doping were grown on each Ge wafer. The 50 nm GaAs layer was expected to be lattice-matched to Ge. The growth was conducted in an Aixtron 2800G4-TM metal-organic chemical vapor deposition (MOCVD) reactor. After the backside SiN deposition and frontside GaAs/$In_{0.015}Ga_{0.985}As$/InGaP layer growth, the thickness before DBR and MQW epitaxy was 376 μm.

The 4-inch GaAs/InGaAs/InGaP/bulk-Ge/SiN wafers were then sent to LandMark for the second MOCVD growth, i.e., the half VCSEL structure epitaxy. A bulk GaAs wafer with 629 μm thickness and 2 degrees off-cut towards <111> was used as the substrate of the control sample for comparison, which LandMark provided. A 500 nm thick GaAs base layer was grown to have a cleaner surface for the subsequent epitaxy. In principle, the n-DBR and MQW layer composition and thickness design of this base layer should be updated according to the Ge substrate lattice constant. However, as this project's goal was to demonstrate the lasing of VCSELs on Ge wafers and preliminary results using a 500 nm GaAs base layer and n-DBR were promising [12], we decided to continue using this design and leave the design update for Ge substrate to future work.

As the target lasing wavelength is 940 nm, the target stopband wavelength of the bottom and the top DBRs is from 915 to 975 nm. The MQW emission wavelength is about 940 nm at the operation temperature of 338 K – 348 K, which is about 920 nm at 298 K. Each DBR consists of 40 periods of n-type doped four layers: 20 nm $Al_xGa_{1-x}As$ (x: 0.12→0.9) with 3×10^{18} cm^{-3} doping / 56 nm $Al_{0.9}Ga_{0.1}As$ with 3×10^{18} cm^{-3} doping / 20 nm $Al_xGa_{1-x}As$ (x: 0.9→0.12) with 2×10^{18} cm^{-3} doping / 49 nm $Al_{0.12}Ga_{0.88}As$ with 2×10^{18} cm^{-3} doping (from the bottom to the top in one period). On top of the DBR, transition layers consisting of 20 nm $Al_xGa_{1-x}As$ (x: 0.12→0.9) with 2×10^{18} cm^{-3} doping / 30 nm $Al_{0.85}Ga_{0.15}As$ with 2×10^{18} cm^{-3} doping were grown before the MQW epitaxy. The MQWs consist of three InGaAs quantum wells with GaAsP barriers. On top of the MQWs, one 100 nm undoped $Al_xGa_{1-x}As$ (x: 0.85→0.3) / 10 nm undoped GaAs are grown as the capping layers. The vapor pressure during growth was 50 mbar, and the growth temperature was set to 760 °C. The sources used for GaAs growth were H_2, SiH_4, AsH_3, and $Ga(CH_3)_3$ (TMGa). During the $Al_xGa_{1-x}As$ growth for bottom DBR layers, $Al_2(CH_3)_6$ (TMAl) was added to provide the Al source. For the MQW growth process, In(CH3)3 (TMIn) and PH3 were the sources to add In and P.

III. Results and Discussions

To investigate the half VCSELs on the 4-inch GaAs/InGaAs/InGaP/bulk-Ge/SiN wafers, optical microscope, atomic force microscope (AFM) imaging, optical reflectance spectra measurements, scanning electron microscopy (SEM) were conducted in the material analysis. Photoluminescence spectroscopy (PL) was measured to characterize the MQW and the flatness of the full 4-inch wafers after the growth was checked by wafer bow and wrap measurement. Secondary ion mass spectrometry (SIMS) was performed to compare the chemical compositions of the QWs and the barrier layers.

A. Surface Quality

Good surface quality was confirmed under the optical microscope and AFM (Fig. 2) for the Ge-based half VCSELs. No cracks and antiphase domains were observed. Fig. 2(b)

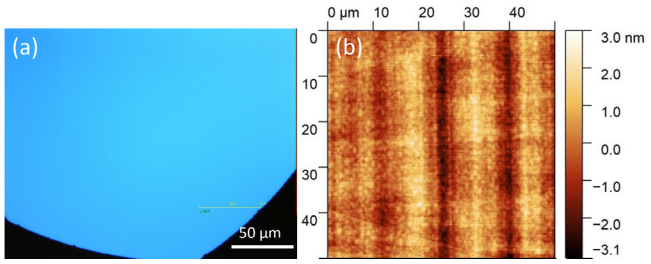

Fig. 2. (a) Surface optical image with 100× magnification and (b) AFM image of Ge-based half VCSELs.

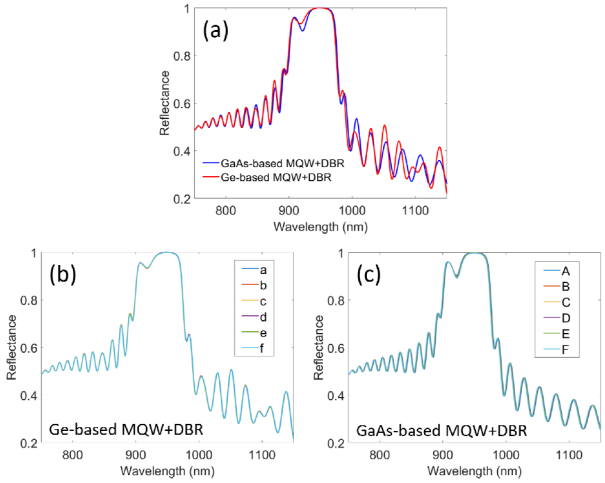

Fig. 3. (a) Normal-incidence reflectance spectra of the GaAs-based half VCSELs and the Ge-based half VCSELs at the center of the wafer. (b) Normal-incidence reflectance spectra of 6 locations of the Ge-based half VCSELs. Spectrum a was measured at the center of the 4-inch wafer. Spectra b – f are across the wafer from the central area to the edge area. (c) Normal-incidence reflectance spectra of 6 locations of the control GaAs-based half VCSELs (a to f) placed from the central area to the edge area.

shows minor crosshatch patterns resulting from the slight lattice mismatches between AlGaAs DBR layers, GaAs, and Ge. The root-mean-square (RMS) roughness measured by AFM for GaAs-based and Ge-based half VCSELs is 0.28 and 0.84 nm, respectively, measured on 50 μm x 50 μm areas, similar to those before MQWs growth [12].

B. Reflectance

The reflectance spectra of GaAs-based and Ge-based half VCSELs were measured with a Filmetrics F40 thin-film analyzer (Fig. 3). All the reflectance values were normalized based on the peak reflectance value of a GaAs-based half VCSEL. The Ge-based half VCSELs have stopband shapes, widths, and maximum peak heights comparable to the GaAs counterpart (Fig. 3(a)). The peak reflectance values of the Ge-based half VCSELs are 99.98% after normalization by the peak GaAs-based half VCSELs reflectance. The dips on the stopband result due to the absorption of the active region. At room temperature, the dip of the stopband of the GaAs-based half VCSELs locates at 922.3 nm, and the Ge counterpart locates at 918.2 nm. The stopband dip positions are consistent with the PL peak wavelength discussed in the following section, as they reflect the energy band gaps of the MQWs.

Good reflectance spectra uniformity across the 4-inch Ge-based half VCSELs is observed in Fig. 3(b), comparable

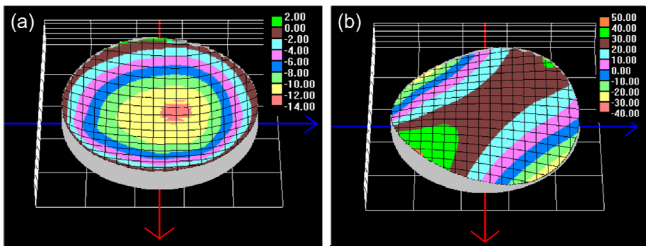

Fig. 4. Bow and warp of (a) the GaAs/InGaAs/InGaP/bulk-Ge/SiN substrate before half VCSELs growth, and (b) the Ge-based half VCSELs. The values of thickness variation across the wafer are based on the reference plane, which is the best fit plane of thickness central plane (Units: μm).

to its GaAs counterpart (Fig. 3(c)). The stopband position shift across the wafer is less than 1.0 nm, and the peak reflectance values are 99.81% to 99.98%. The slight shift of stopband position and fluctuation of peak reflectance values are expected due to flatness variation across the 4-inch wafer (Fig. 4).

The bow and warp of the Ge wafer before and after the half VCSEL growth were measured by the Tropel C100 system. The average distance from the reference plane before and after the growth are 13.32 and 73.88 μm, respectively. The concave bow of the pre-growth wafer (Fig. 4(a)) resulted from the tensile stress brought by the GaAs capping layer with a smaller lattice constant (5.653 Å) than the Ge lattice constant (5.658 Å). With MQWs, the shape turned to be more convex (Fig. 4(b)), due to InGaAs's much larger lattice constant (5.743 Å).

C. PL Measurements

PL measurement was conducted at room temperature 298 K to characterize the light emission from the MQWs (Fig. 5). The PL system is equipped with a 532 nm continuous-wave laser and a liquid nitrogen Ge PIN diode detector made by Bruker Ltd. The spectra of both half VCSELs share comparable peak intensity with a difference of $< 0.2\%$. The PL peak positions of the Ge- and GaAs-based half VCSEL are 918.865 and 923.419 nm, respectively. The 4.55 nm peak wavelength shift translates to a 6.66 meV difference in the corresponding photon energy. This may be caused by the composition and strain variation in the MQWs, which were then investigated by SEM and SIMS, as discussed below. For the PL uniformity across the full wafer, the Ge-based half VCSELs show an 8.54% intensity non-uniformity (1.04% in the GaAs-based counterpart) and a 0.028% peak wavelength non-uniformity (0.014% in the GaAs-based counterparts). Due to time and resource constraints, the growth process of the active structure and DBR was previously developed for the growth on GaAs wafers and had not been optimized for the growth on Ge wafers.

D. Cross-Sectional SEM Images

The half VCSELs cross-sections were observed by SEM. Before measurement, a diamond scriber cleaved the SEM samples from the half VCSEL wafers. A FEI Nova NanoSEM system collected the SEM images.

Good periodicity and layer uniformity of both types of structures can be confirmed (Fig. 6). The thickness of MWQs

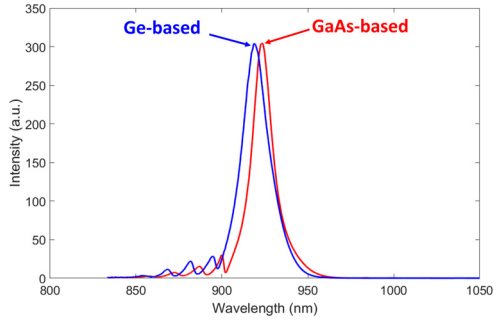

Fig. 5. Photoluminescence spectra of the GaAs-based half VCSELs and the Ge-based half VCSELs.

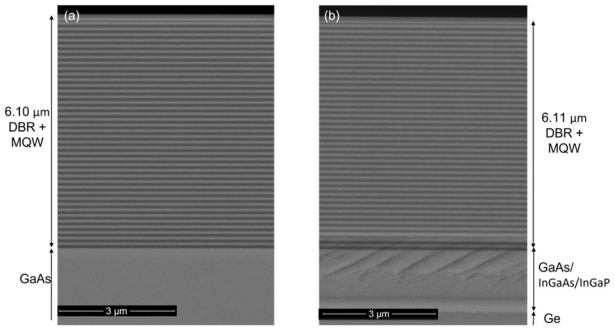

Fig. 6. Cross-section SEM images at 30K× magnifications of a (a) bulk GaAs-based half VCSELs, (b) Ge-based half VCSELs.

was too thin to be measured accurately by SEM. The total thickness of the Ge-based half VCSELs is 6.11 μm, which is in good agreement with the 6.10 μm thickness of the GaAs counterpart. This thickness difference was insufficient to explain the 6.66 meV difference in peak PL photon energy.

E. SIMS Measurement

SIMS was performed to check the molar fractions of Al, Ga, As, P, and Indium (In) of the MQWs and barrier layers. The measurement was conducted by Eurofins EAG Laboratories. The accuracy of atom fractions is about +/− 5% in the AlGaAs layer and about +/− 20% in the mixed As/P layers.

Atomic fractions of In in the Ge- and GaAs-based MQWs are very close and are within the SIMS accuracy. In the top and bottom GaAsP barrier layers, the Ge-based sample has around 3% more P than the GaAs-based sample, corresponding to a bandgap difference of 0.039 eV and a 0.18% strain difference. The 3% P difference was expected, considering the epitaxy growth rate on Ge and GaAs wafers in the same batch was slightly different due to the different material, thickness, and thermal conductivity. These differences resulted in the stopband dip wavelength shift in Fig. 3(a) and the peak wavelength shift in the PL spectrum in Fig. 5. Those spectra of Ge-based half VCSELs shift to a shorter wavelength.

F. Future Work

The results from the half VCSELs growth are very encouraging. The subsequent growth of full VCSEL epitaxy on 4-inch Ge wafers was just performed, and the calibration runs to tune the Ge-VCSELs growth recipe to have the 940 nm lasing wavelength were successful. More material analysis and device performance measurements will be conducted and reported in separate letters.

IV. Conclusion

We independently developed a bulk-Ge-based half VCSEL technology, and this report revealed many key technology details which are not available in the literature. Even without any process optimization for Ge substrates, the Ge-based half VCSELs have uniform reflectance spectra, comparable PL peak intensity, and peak shape to those grown on the bulk GaAs wafer. Sub-nm RMS surface roughness and uniform DBR and MQWs growth across the wafer were achieved. No APDs or cracks were formed in epitaxy on Ge wafers. Our promising results strongly support the full VCSEL growth and fabrication on larger-area bulk Ge substrates for the mass production of AlGaAs-based VCSELs.

Acknowledgment

Umicore NV, Belgium, is recognized for providing bulk Ge wafers with GaAs/InGaAs/InGaP epitaxy layers and SiN back coating.

References

[1] A. Extance, “Faces light up over VCSEL prospects,” SPIE Newsroom, Apr. 9, 2018. [Online]. Available: https://www.spie.org/news/spie-professional-magazine-archive/2018-april/faces-light-up-over-vcsel-prospects

[2] M. Dummer, K. Johnson, S. Rothwell, K. Tatah, and M. Hibbs-Brenner, “The role of VCSELs in 3D sensing and LiDAR,” *Proc. SPIE*, vol. 11692, Mar. 2021, Art. no. 116920C.

[3] K. Iga, “Surface-emitting laser-its birth and generation of new opto-electronics field,” *IEEE J. Sel. Topics Quantum Electron.*, vol. 6, no. 6, pp. 1201–1215, Nov. 2000.

[4] Yole Development, *VCSEL—Technology and Market Trends 2022 Report*, Yole Intell., Lyon, France, 2022.

[5] D. Wiedenmann, M. Grabherr, R. Jager, and R. King, “High, volume production of single-mode VCSELs,” *Proc. SPIE*, vol. 6132, Feb. 2006, Art. no. 613202.

[6] J. Baker et al., “Impact of strain-induced bow on the performance of VCSELs on 150 mm GaAs- and Ge-substrate wafers,” *Proc. SPIE*, vol. 12141, May 2022, Art. no. PC1214108.

[7] F. Adel Ismael Chaqmaqchee and J. A. Lott, “Impact of oxide aperture diameter on optical output power, spectral emission, and bandwidth for 980 nm VCSELs,” *OSA Continuum*, vol. 3, no. 9, p. 2602, 2020.

[8] C. Bocchi, C. Ferrari, P. Franzosi, A. Bosacchi, and S. Franchi, “Accurate determination of lattice mismatch in the epitaxial AlAs/GaAs system by high-resolution X-ray diffraction,” *J. Cryst. Growth*, vol. 132, pp. 427–434, Sep. 1993.

[9] M. Bosi and G. Attolini, “Germanium: Epitaxy and its applications,” *Prog. Crystal Growth Characterization Mater.*, vol. 56, nos. 3–4, pp. 146–174, Sep. 2010.

[10] B. Depuydt, A. Theuwis, and I. Romandic, “Germanium: From the first application of Czochralski crystal growth to large diameter dislocation-free wafers,” *Mater. Sci. Semicond. Process.*, vol. 9, nos. 4–5, pp. 437–443, Aug. 2006.

[11] A. Johnson et al., “High performance 940 nm VCSELs on large area germanium substrates: The ideal substrate for, volume manufacture,” *Proc. SPIE*, vol. 11704, Mar. 2021, Art. no. 1170404.

[12] Y. Zhao et al., “Monolithic integration of 940 nm AlGaAs distributed Bragg reflectors on bulk Ge substrates,” *Opt. Mater. Exp.*, vol. 12, no. 3, pp. 1131–1139, 2022.